Monomer−Dimer Equilibria of Oxo/Imido Complexes of Heptavalent Rhenium: Theoretical and Spectroscopic Investigations

Philip Gisdakis,[a] Notker Rösch,*[a] Éva Bencze,[b,c] Janos Mink,[c,d] Isabel S. Gonçalves,[e] and Fritz E. Kühn*[b]

Keywords: Density-functional calculations / Imido ligands / Oxygen bridges / Rhenium / Transition states

Mixed oxo/imido derivatives of methyltrioxorhenium(VII) form dimers in the solid state at ambient temperature. Density-functional calculations show that the dimerization is exothermic. The most stable derivatives were calculated to display a pseudo trigonal-bipyramidal coordination with two bridging oxygen centers and the methyl groups in a *trans* arrangement. This configuration is energetically more favored than a *cis* arrangement of the methyl groups and a pseudo square-pyramidal structure at the metal centers. In the case of methyltrioxorhenium(VII), the dimerization is slightly endothermic, even for the optimal dimeric structure, so that dimers cannot be isolated. However, there is evidence for the transient existence of oxygen bridges between methyltrioxorhenium(VII) in solution. For mixed imido/oxo species, oxygen bridging is observed in all cases of dimerization; results of thermogravimetric/mass spectrometric studies demonstrate that these bridging dimers are weakly bound. From vibrational spectroscopic analysis, there is no evidence for nitrogen-bridged homologues. The density-functional calculations show that imido groups form bridges only in the case of sterically undemanding ligands. However, these complexes are too unstable to be isolated.

Introduction

Organorhenium(VII) oxides have been studied in great detail in recent years. The use of some derivatives, most prominently methyltrioxorhenium(VII), as catalysts in a broad range of reactions[1] triggered a significant amount of investigations,[2] among them several theoretical studies.[3] However, far less investigations have been devoted to organorhenium(VII)imido compounds. Very few studies concerning their synthesis, structures, and spectroscopic properties have been carried out in the last two decades.[2a,4] Recently, we discovered a temperature-dependent monomer−dimer equilibrium that occurs in solution in the case of mixed oxo/imido Re^{VII} complexes.[5] However, the ability of mixed oxo/imido complexes to form dimers may provide more insight into the propensity of methyltrioxorhenium(VII) to polymerize. It is important to remember that the first polymeric organometallic oxide ever described was formed from methyltrioxorhenium(VII).[6] To date, the manner in which the polymerization of methyltrioxorhenium(VII) starts or which intermediates are formed remain open to discussion since dimeric or oligomeric units have never been isolated or observed in situ. Therefore, it is of interest to compare methyltrioxorhenium(VII) with closely related complexes in which some or all of the oxygen ligands are replaced by imido groups, in order to examine conditions that would enable dimeric methylrhenium(VII) oxo complexes to be isolated. The energy differences between oxo/imido complexes and pure oxo complexes are of particular interest in this respect.

It is worth noting that isolated dimeric methylrhenium(VII) oxo/imido complexes have been observed to exhibit structural features[5] that differ from those predicted for hypothetical dimeric methyltrioxorhenium(VII) based on Hartree−Fock self-consistent field calculations using a relativistic effective core potential.[6c] In this context, a recent computational study focused on the thermochemistry of the Re−oxo bond cleavage in complexes of the type $LReO_3$, with L = Cp, Cp*, CH_3, C_6H_5, and others.[7] The Re−O bond-dissociation energy was found to depend quite strongly on the nature of the ligand L. A comparison of the calculated results with experimental data demonstrated the convincing accuracy of the applied computational method, a hybrid density-functional approach, and hence the opportunity for a computational study of organometallic thermochemistry.

Another point of interest in recent literature reports is the ability of methyltrioxorhenium(VII) and related complexes to easily exchange their terminal oxygen ligands. This has been shown by ^{17}O NMR spectroscopic studies[8] and it has been assumed that this process proceeds through oxy-

[a] Institut für Physikalische und Theoretische Chemie, Technische Universität München,
Lichtenbergstraße 4, 85747 Garching, Germany
[b] Anorganisch-Chemisches Institut der Technischen Universität München,
Lichtenbergstraße 4, 85747 Garching bei München, Germany
[c] Institute of Isotope and Surface Chemistry of the Hungarian Academy of Sciences,
P. O. Box 77, 1525 Budapest, Hungary
[d] Department of Analytical Chemistry, University of Veszprém, Egyetem UTCA 10, P. O. Box 158, 8203 Veszprém, Hungary
[e] Departamento de Química, Universidade de Aveiro, Campus de Santiago, 3800 Aveiro, Portugal

  1434−1948/01/0404−0981 $ 17.50+.50/0

gen bridges. However, the existence of energetically accessible dimeric states that allow oxygen exchange through such bridges is still unclear.

In the present work, we perform a detailed theoretical study of the monomer−dimer equilibria that occur in the case of mixed methylrhenium(VII) oxo/imido species and we compare them to dimers of pure oxo and imido derivatives. The theoretical study is supplemented by thermogravimetric/mass spectrometric investigations of the sublimation behavior of selected complexes of this type and a detailed IR/Raman study of monomeric and dimeric oxo/imido methylrhenium(VII) complexes.

Results and Discussion

Dimer Systems

We start with an overview of the various monomers and dimers to be studied. From the monomeric compound CH_3ReO_3 (**1**) one can derive the monomers of interest if one successively substitutes oxo functions by imido groups to yield $CH_3ReO_2(NR)$ (**2**), $CH_3ReO(NR)_2$ (**3**), and $CH_3Re(NR)_3$ (**4**). In the computational investigation, we used two imido groups with R = H (**a**) and CH_3 (**b**), while for the experimental characterization we employed the (2,6-diisopropylphenyl)imido ligand (**c**) (see Scheme 1). Such a relatively bulky ligand is required to guarantee the sufficient stability of the product complexes. Accordingly, the hydrogen compound $CH_3ReO_2(NH)$ is referred to as **2a**, whereas **2b** designates the corresponding methylated compound $CH_3ReO_2(NCH_3)$. We proceeded in the same way with the bis- and tris(imido) complexes $CH_3ReO(NR)_2$ and $CH_3Re(NR)_3$. The experimentally characterized and therefore most stable dimer structures of the monomers **2c** and **3c** are denoted as **5c** and **6c**, respectively. We will begin by analyzing different isomeric structures of the analogous H- and CH_3-ligated systems **5a/b** and **6a/b** and later on will introduce a more detailed nomenclature for describing these different structures.

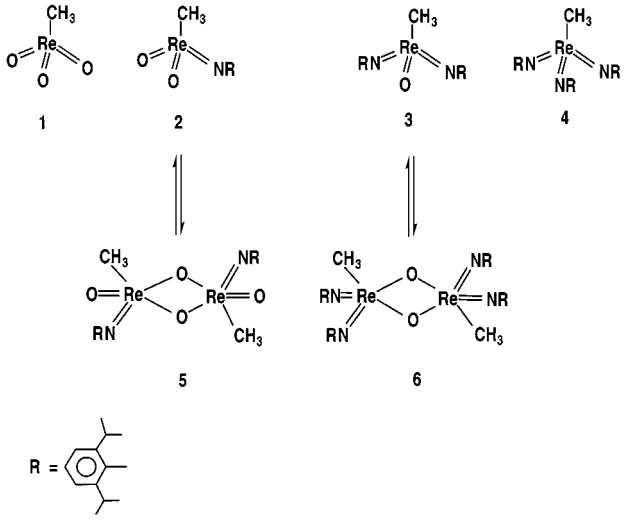

Scheme 1

In the computational study we focused on homogenous dimers, i.e. dimers that consist of two equal monomeric units of **1**, **2a/b**, and **3a/b**. We also studied two mixed dimers, composed of two different monomers. The complexes can only dimerize as two fundamental structural types: a pseudo trigonal-bipyramidal coordination [**A**, see Figure 1, (a) and (b)] and a pseudo square-pyramidal coordination of the rhenium center [**B**, see Figure 1, (c) and (d)]. In the latter case, two terminal and two bridging ligands form the basis of a square pyramid, while the methyl ligand defines its top. Structures **A** and **B** may each occur with a *cis* and *trans* orientation of the CH_3 ligand. Furthermore, we need

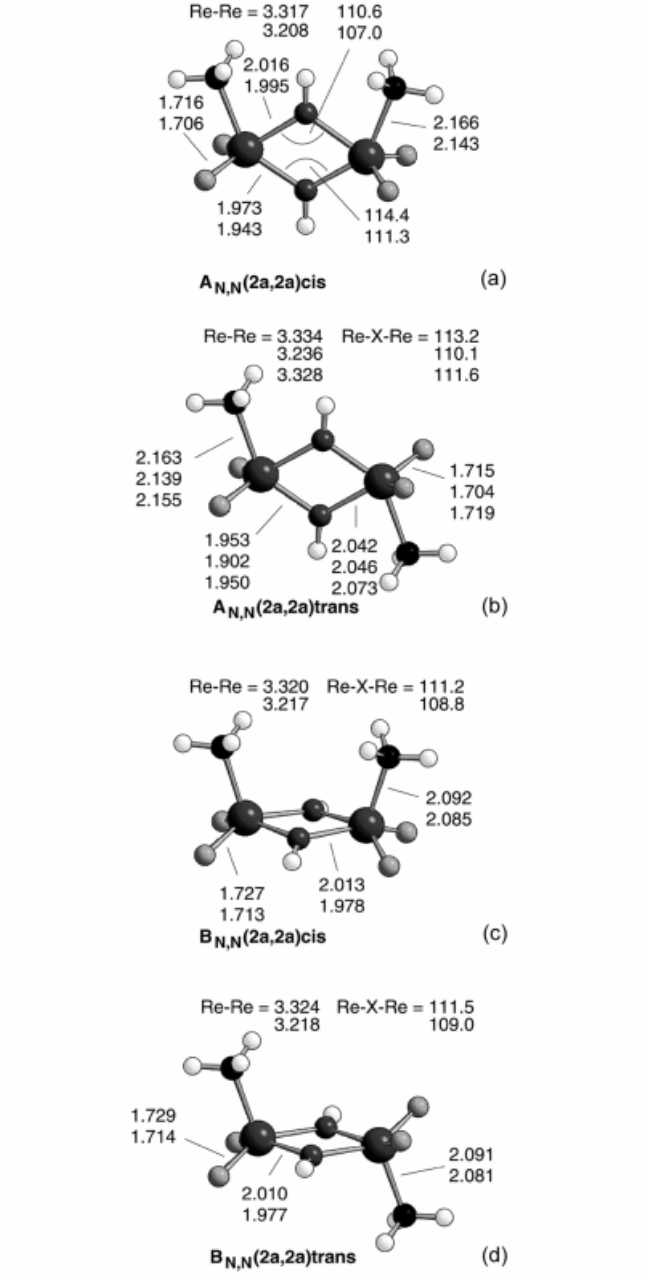

Figure 1. Calculated structures of homogeneous dimers of **2a** with bridging nitrogen centers; pertinent calculated structure parameters (bond lengths in Å, angles in °) of the corresponding dimers of **2a**, **1**, and **2b** listed in columns in that order

to indicate the bridging atoms X (O and/or N) of the imido complexes **2** and **3** and of the mixed dimers. For this purpose, we add the bridging atoms as subscripts. For instance,

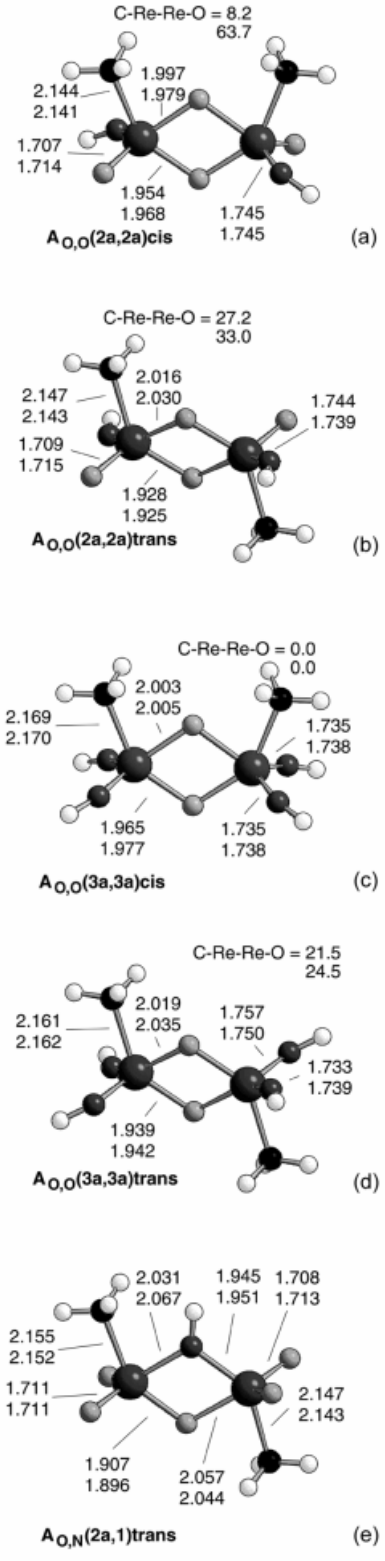

Figure 2. Calculated structures of homogeneous dimers of **2a** and **3a** with bridging oxygen centers and of the mixed O-bridged/N-bridged dimer (**2a**,**1**); pertinent calculated structure parameters (bond lengths in Å, angles in °) of the corresponding dimers of **2a** and **2b** or **3a** and **3b** in columns in that order

complex $\mathbf{A_{N,N}(2a-2a)cis}$ exhibits a trigonal-bipyramidal conformation (structure **A**) with two N atoms bridging two **2a** monomers in which the two methyl groups adopt a *cis* orientation.

In Figure 1 and Figure 2 we display various structures of dimers (**2a**,**2a**), (**3a**,**3a**), and (**2a**,**1**). Inspection of the calculated vibrational data reveals that, with one (partial) exception, all structures **A** correspond to local minima, whereas structures **B** represent transition structures (see below). The exceptional case $\mathbf{A_{N,N}(2b-2b)trans}$ features two vibrational modes with imaginary frequencies that correspond to rotational motions of the methyl substituents at the nitrogen centers; thus, even in this case, the remaining framework of the dimer represents a local-minimum structure.

Structural Properties

In Figure 1, featuring the homogeneous dimer of **2a** with bridging imido groups, we also present characteristic bond lengths and angles of dimers of **1** and **2b** in compact column form: values in the first line of each column refer to dimers with bridging NH groups (monomer **2a**). Values in the second line refer to dimers of the monomer **1**. Where present, values in the third line refer to dimers with bridging NCH_3 groups (monomer **2b**). To facilitate the calculations, symmetry constraints have been employed, resulting in idealized dimer structures (see below). The *cis* complexes [C_{2v} symmetry for **1** and **2a**; Figure 1, (a) and (c)] exhibit a mirror plane perpendicular to the carbon−rhenium plane, containing the bridging atoms, while the *trans* structures feature an inversion center [C_{2h} symmetry for **1** and **2a**; Figure 1, (b) and (d)]. In type **B** structures, the Re−X bonds are equivalent by symmetry, while type **A** structures exhibit two shorter and two longer Re−X bonds. Each bridging atom of complex $\mathbf{A_{X,X}(Y-Y)cis}$ is symmetrically located between the rhenium atoms and both Re−X bonds are of equal length. In complexes $\mathbf{A_{X,X}(Y-Y)trans}$ with two different Re−X bond lengths, each bridging atom X may be assigned to one of the two rhenium centers; the Re−X bond located closer to the methyl ligand is shorter.

Energetics

One goal of the computational study was to determine the most stable dimeric structures of MTO and of related imido complexes (Table 1). As models for the whole class of systems, we first calculated the formation energies of the dimers of MTO **1** and of the N-bridged dimers of the mono(imido) derivative **2a** of MTO, for both fundamental structure types **A** and **B** and different orientations of the methyl groups. In the next step, the most stable structures determined in this way were then also studied for the dimers of **2b**, **3a**, and **3b**. To assist in assessing the relative energies of the various configurations, the dimerization energies are compared in Figure 3. The formation of dimers $\mathbf{B_{O,O}(1-1)cis}$ and $\mathbf{B_{O,O}(1-1)trans}$, displaying a square-pyramidal coordination, from two MTO monomers is more endothermic (by 35.5 and 32.2 kcal/mol, respectively) than that of the corresponding type **A** dimers $\mathbf{A_{O,O}(1-1)cis}$ and

$A_{O,O}$(1−1)trans with a trigonal-bipyramidal coordination (by 5.8 and 1.7 kcal/mol, respectively). The *trans* configurations are more stable than the corresponding *cis* forms by 3−4 kcal/mol. It is worth noting that the differences in stability between the **A** and **B** forms are very similar for both *cis*/*trans* isomers. **$A_{O,O}$(1−1)cis** is more stable than **$B_{O,O}$(1−1)cis** by 29.7 kcal/mol; the corresponding energy difference of the *trans* complexes is 30.5 kcal/mol. For the most stable dimer **$A_{O,O}$(1−1)trans**, we also calculated that the enthalpy of formation (at T = 298.15 K) is larger than the dimerization energy by 1.7 kcal/mol (Table 1).

Table 1. Calculated results of dimerization energies ΔE and selected dimerization enthalpies ΔH (in kcal/mol)

	ΔE	ΔH
MTO dimers:		
$A_{O,O}$(1−1)cis	5.78	
$A_{O,O}$(1−1)trans	1.74	3.47
$B_{O,O}$(1−1)cis	35.54	
$B_{O,O}$(1−1)trans	32.21	
N-Bridged mono(imido) dimers:		
$A_{N,N}$(2a−2a)cis	−7.68	
$A_{N,N}$(2a−2a)trans	−9.34	−5.07
$B_{N,N}$(2a−2a)cis	17.97	
$B_{N,N}$(2a−2a)trans	20.08	
$A_{N,N}$(2b−2b)trans	12.38	13.39
Terminal mono(imido) dimers:		
$A_{O,O}$(2a−2a)cis	4.19	
$A_{O,O}$(2a−2a)trans	−1.15	4.10
$A_{O,O}$(2b−2b)cis	−0.33	
$A_{O,O}$(2b−2b)trans	−2.50	−1.04
Terminal bis(imido) dimers:		
$A_{O,O}$(3a−3a)cis	5.43	
$A_{O,O}$(3a−3a)trans	1.44	3.04
$A_{O,O}$(3b−3b)cis	0.68	
$A_{O,O}$(3b−3b)trans	−1.81	0.36
N-Bridged tris(imido) dimers:		
$A_{N,N}$(4a−4a)trans	−5.03	
$A_{N,N}$(4b−4b)trans	10.30	
Mixed dimers:		
$A_{O,N}$(1−2a)trans	−4.85	
$A_{O,N}$(1−2b)trans	4.23	

A similar stability trend was found for the N-bridged dimers of **2a**. Type **A** structures are more stable than type **B** structures. For **A**, the *trans* orientation of the methyl group is also more stable than the *cis* configuration: the dimerization energy was calculated to be −9.3 kcal/mol for **$A_{N,N}$(2a−2a)trans** and −7.7 kcal/mol for **$A_{N,N}$(2a−2a)cis.** However, the *cis*/*trans* energy difference, 1.6 kcal/mol, is only half as large as for the corresponding dimers of MTO. Note that for type **B** structures (square-pyramidal coordination of Re), the *cis*/*trans* preference is reversed. **$B_{N,N}$(2a−2a)cis** is less endothermic than **$B_{N,N}$(2a−2a)trans** with dimerization energies of 18.0 and 20.1 kcal/mol, respectively. This finding is a consequence of the symmetry constraints employed in the calculations. In the *trans* complex (C_{2h} symmetry), the imido H atom is unable to bend outside the Re−N−Re plane, as it can in the case of the *cis* orientation in which the H atom bends downwards (Figure 1). However, the **A**/**B** energy difference for the *trans* isomers (29.4 kcal/mol) is very similar to that of MTO dimers (29.7 kcal/mol for *cis* and 30.5 kcal/mol for *trans*). For the *cis* dimers of **2a**, the **A**/**B** energy difference is significantly reduced (25.7 kcal/mol) since **$B_{N,N}$(2a−2a)cis** is more stable than **$B_{N,N}$(2a−2a)trans**.

In contrast to the results obtained for the MTO dimers, the N-bridged dimers of **2a** feature exothermic dimerization energies for type **A** structures. For the most stable isomer **$A_{N,N}$(2a−2a)trans** we also calculated the enthalpy of dimerization (−5.1 kcal/mol, Table 1), which is less exothermic than the corresponding dimerization energy by 4.3 kcal/mol. Substitution of the bridging imido H atom by a methyl group in the most stable dimer **$A_{N,N}$(2a−2a)trans** leads to the congener **$A_{N,N}$(2b−2b)trans** and renders the dimerization endothermic (12.4 kcal/mol). This is due to steric hindrance, but electronic effects are also probably involved since the energy difference due to methylation (21.7 kcal/mol) seems to be too high to be caused by steric hindrance only. The dimerization enthalpy of **$A_{N,N}$(2b−2b)trans** is larger than the corresponding energy difference (1 kcal/mol, Table 1).

The fundamental structure type **A** (trigonal-bipyramidal coordination) with a *trans* orientation of the methyl groups yields the most stable structures of the O-bridged [**$A_{O,O}$(1−1)trans**] as well as of the N-bridged dimers [**$A_{N,N}$(2a−2a)trans**] of MTO and its imido derivatives. While the energy differences between corresponding complexes of structures **A** and **B** is about 30 kcal/mol, the *cis*/*trans* energy difference is approximately only 1−3 kcal/mol. Therefore, in the following we will focus on trigonal-bipyramidal complexes **A**, but we will continue to compare *cis* and *trans* isomers.

Substitution of two terminal oxo groups (one per monomer) in MTO dimers **$A_{O,O}$(1−1)cis/trans** by imido groups (NH in the case of monomer **2a** and NCH_3 in the case of monomer **2b**) leads to **$A_{O,O}$(2a−2a)cis/trans** and **$A_{O,O}$(2b−2b)cis/trans** (see Figure 2). The *cis* compounds were calculated with C_2 symmetry, while the *trans* configurations may be studied with a C_i-symmetry constraint. This substitution results in dimer formation becoming exothermic or at least less endothermic [**$A_{O,O}$(2a−2a)cis**]; in the case of the **2a** dimers, the dimerization energies change by −1.6 and −2.9 kcal/mol for *cis* and *trans* configurations, respectively, and even more so in the case of the **2b** dimers, by −6.1 and −4.2 kcal/mol for *cis* and *trans* configurations, respectively (Table 1). The energy preference between the more stable *trans* isomers is reversed at the enthalpy level: **$A_{O,O}$(2b−2b)trans** is estimated to be the only stable homogeneous dimer with terminal mono(imido) complexes.

Substitution of all four terminal oxo groups of **$A_{O,O}$(1−1)cis/trans** by imido ligands leads to the O-bridged dimers of the bis(imido) derivatives of MTO, **$A_{O,O}$(3a−3a)cis/trans** and **$A_{O,O}$(3b−3b)cis/trans**. The *cis* dimers were calculated with C_{2v} symmetry, while the *trans* compounds were calculated with C_i symmetry. Among these oxygen-bridged dimers with two terminal amido group, **$A_{O,O}$(3b−3b)trans** is estimated to exhibit the least endothermic enthalpy of formation (Table 1). In general, the formation energies of these dimers are larger than those of the corresponding mono(imido) compound dimers, but still lower than those of the corresponding dimers of MTO

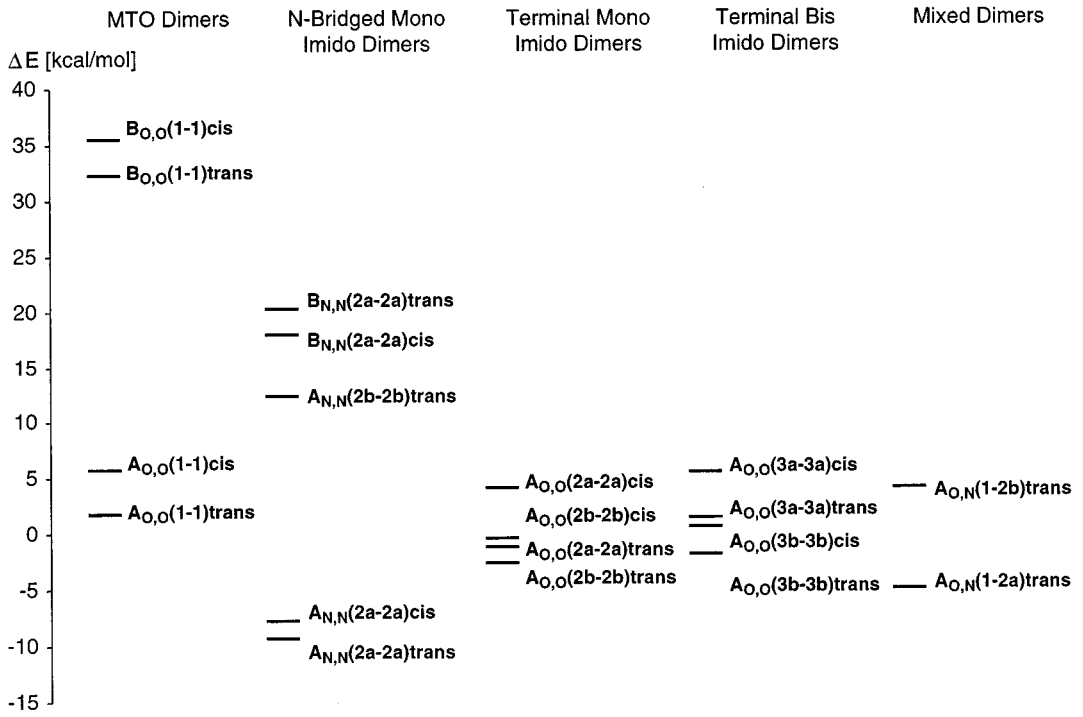

Figure 3. Calculated dimerization energies ΔE of various structures [MTO = methyltrioxorhenium(VII)]

(Figure 3). Just as in the case of the mono(imido) compounds, methyl substituents at the N atoms render dimer formation less endothermic. Substitution of the bridging oxygen centers of $\mathbf{A_{O,O}(3a-3a)trans}$ by NH groups leads to $\mathbf{A_{N,N}(4a-4a)trans}$; in this way, the dimerization energy is reduced by 6.5 kcal/mol, rendering the process exothermic (Table 1). On the other hand, the analogous substitution by NCH_3, resulting in the dimer $\mathbf{A_{N,N}(4b-4b)trans}$, changes the dimerization energy by 12.1 kcal/mol and renders the dimerization notably endothermic.

Mixed dimers provide more insight into the energy situation, since they feature one O and one NH bridge and are therefore intermediate between the dimeric structures of **1** and **2**. In these mixed dimers MTO, dimerizes with **2a** to form O,N-bridged $\mathbf{A_{O,N}(1-2a)trans}$ or with **2b** to form $\mathbf{A_{O,N}(1-2b)trans}$. Stated differently, if one substitutes one bridging oxygen center of the MTO dimer $\mathbf{A_{O,O}(1-1)trans}$ by NH, the dimerization energy changes by −6.6 kcal/mol and dimer formation becomes exothermic by −4.9 kcal/mol. Further substitution of the second bridging oxygen atom, leading to $\mathbf{A_{N,N}(2a-2a)trans}$ renders the formation even more exothermic with a change in the energy of dimer formation of −4.5 kcal/mol. In the case of NCH_3 the situation is reversed: substitution of the first imido renders dimer formation more endothermic by 2.5 kcal/mol and substitution of the second one even more so, by 8.2 kcal/mol.

In summary, substitution of one terminal oxo group of each monomer by an imido group renders dimer formation less endothermic or even exothermic. Substitution of the second terminal oxo group leads to a dimer stability in between that of MTO dimers and its mono(imido) derivatives. Compounds containing terminal NCH_3 groups always yield more stable dimers than NH imido complexes. Mixed O- and NH-bridged dimers exhibit dimer formation energies between those of purely O-bridged and purely NH-bridged complexes, while the mixed O- and NCH_3-bridged dimer forms more readily than the purely NCH_3-bridged dimer. These results suggest that NH groups in bridging positions render dimer formation more favorable, while NCH_3 imido complexes do so in terminal positions. In fact, imido groups with larger carbon substituents will not assume bridging positions.

Structurally, the dimerization reaction is an addition of two Re=O (Re=NR) bonds, resulting in a substitution of one Re=O (Re=NR) double bond by two Re−O (Re−NR) single bonds. One thus expects that the dimerization energy is controlled by the strength of the Re=O (Re=NR) bond.[7] To analyze this effect, we calculated the reaction energy for the monomeric compounds **1**, **2a/b**, and **3a/b**, when water is added to the rhenium−oxo bond, resulting in $Re(OH)_2$ moieties. In addition to model N-bridged dimerization, we calculated the energy of the addition of water to the Re=NR units of **2a/b**, which results in the formation of Re(OH)(NHR) moieties. Figure 4 demonstrates a linear correlation of these reaction energies of water addition with the most endothermic (or least exothermic) dimerization energies; only $\mathbf{A_{N,N}(2b-2b)trans}$ and $\mathbf{A_{N,N}(4b-4b)trans}$ give rise to exceptions. The more stable the product of water addition, the more exothermic is the dimerization. In $\mathbf{A_{N,N}(2b-2b)trans}$, the large endothermicity is due to the steric repulsion between the *N*-methyl groups and the methyl groups coordinated at the rhenium centers. As judged by the energy of water addition, the intrinsic dimerization energy should be comparable to that of MTO [$\mathbf{A_{O,O}(1-1)trans}$].

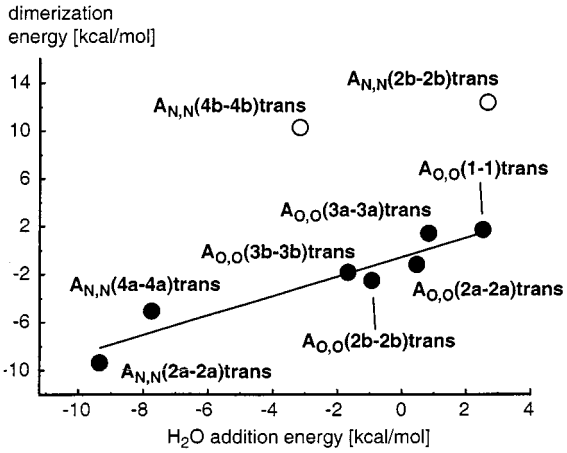

Figure 4. Calculated dimerization energies as function of the calculated energies of the addition of H_2O to an Re=X bond of the corresponding monomers

Thermogravimetry and Mass Spectrometry (TG-MS)

We now turn to a discussion of the dimerization process based on experimental information. We anticipated that two different features should influence the sublimation points of the complexes **1**−**4**: (i) the dimerization of compounds **2c** and **3c** by oxygen bridges (to yield **5c** and **6c**); and (ii) the increasing weight of the monomers due to successive replacement of terminal oxo ligands by bulky imido groups. The relative importance of these independent factors can be convincingly demonstrated by TG-MS examinations. The thermal behavior of CH_3ReO_3 (**1**) has already been reported.[9] This compound already begins to sublime below 50 °C; no decomposition is evident even after complete sublimation. These compounds are less volatile because of the weight increase due to the bulky imido ligands, and the dimerization to form compounds **5c** and **6c** at ambient temperatures. Therefore, they sublime at significantly higher temperatures than compound **1**. For **5c** and **6c**, sublimation is observed to start at 76.75 and 157.08 °C, respectively. The complexes sublime completely, and no residues remain. Mass spectrometry of the gas phase shows no traces of the dimeric species **5c** and **6c**, only the monomers **2c** and **3c** are observed. The sublimed compounds crystallize immediately on colder parts of the thermobalance. NMR and IR spectroscopy of the crystallized compounds clearly shows that dimers **5c** and **6c** have been reformed. The onset of the sublimation of complex **4c** is at 193.48 °C. As expected, no dimer is observed in the gas phase, whereas NMR and IR spectroscopy of the sublimed complex indicates the presence of the original dimer complex. No residue remains after the sublimation, confirming that decomposition does not take place. The changes in the temperature at which sublimation of complexes **1**, **4c**, **5c**, and **6c** starts evidently depends only on the molecular mass of the monomer and increases in accordance with the increasing number of the heavy imido ligands from < 50°C in **1** to nearly 200 °C in **4c**. These observations show that the energy which is necessary to monomerize complexes **5c** and **6c** must be relatively small and that the Re−O−Re bridges are weak. This is in good agreement with the computational results on the Re−O−Re bond strength described above and with observations made in solution.[5] Since all compounds examined display a dimerization energy of less then 5 kcal/mol, it is not surprising that Re−O−Re bonds break readily at the observed temperatures.

Vibrational Properties of the Dimers

The structures of the monomers under investigation belong to the C_{3v} (**1** and **4c**) and C_{2h} (**5c** and **6c**) symmetry groups or can be idealized such that these symmetry assignments hold. Characteristic vibrations are given in Table 2. Complex **4c** shows a strong analogy with compound **1**.[10] The only important difference in this context is observed for the $Re(=N)_3$ stretching vibrations which are assigned to the bands at 1333 cm^{-1} and 1290 cm^{-1} for the asymmetric and symmetric modes, respectively (calculated at 1268 cm^{-1} and 1311 cm^{-1} for **4b** and at 943 cm^{-1} and 971 cm^{-1} for **4a**, see below). The vibrations of the $[CH_3-Re]$ moiety are characteristic for all species examined. It is clear that the IR and Raman bands alternate, especially for the Re−O−Re and the $Re-CH_3$ skeletal stretching modes. This finding indicates the existence of an inversion center for the dimeric compounds. The mutual-exclusion rule is even more pronounced for low-frequency skeletal deformational modes (below 500 cm^{-1}, see Table 2).

There is no strong Raman band in the low-frequency region that can be assigned unambiguously to an Re−Re stretching mode. Accordingly, the dimeric compounds should have a bridging structure. The Re−Re bond lengths of **5c** and **6c** were determined experimentally to be 3.090(1) Å and 3.1190(3) Å, respectively;[5] the corresponding calculated values of the analogous methyl-ligated dimers of **2b** and **3b** [actually in configurations **$A_{O,O}$(2b−2b)trans** and **$A_{O,O}$(3b−3b)trans**, see below] are 3.18 Å and 3.20 Å, respectively. Therefore, the Re−Re interaction cannot be fully ignored, but the metal−metal interaction are probably very weak. For comparison, we mention that the Re−Re distance in the hypothetical dimer $(CH_3ReO)_2(\mu\text{-}O)_2$ of the Re^V species CH_3ReO_2 was calculated to be 2.59 Å. The metal−metal distance in the corresponding dimer $(CpReO)_2(\mu\text{-}O)_2$ of the species $CpReO_3$ was calculated to be 3.14 Å.[7] On the other hand, the Re−Re distance of the experimentally characterized dimer $[(CH_3)_2Re^{VI}O]_2(\mu\text{-}O)_2$ is 2.593(<1) Å[11] and that of $(Cp^*ReO)_2(\mu\text{-}O)_2$ is 3.143(<1) Å.[12]

On the basis of experimental IR and Raman spectroscopy, and the calculated dimerization energies, we conclude that there are no N-bridged dimers with bulky substituents on the nitrogen atom. All dimers are expected to feature bridging oxygen atoms. Experimental characterization of the vibrations of N-bridged dimers is thus not possible. For the oxygen-bridged dimers, two characteristic bands near 725 cm^{-1} and 695 cm^{-1} were assigned to Re−O−Re stretching modes. These Re−O−Re stretching vibrations have a lower intensity in solution spectra. There are no indications pointing to the formation of Re−N−Re bridges, neither in the solid state, nor in solution. However,

Table 2. Selected structurally characteristic IR and Raman frequencies in the range 3000−500 cm^{-1}, and full spectra below 500 cm^{-1}

CH_3ReO_3 (**1**)[a]		$[CH_3ReO_2(NR)]_2$ (**5c**)		$[CH_3ReO(NR)_2]_2$ (**6c**)		$CH_3Re(NR)_3$ (**4c**)		Assignments	Sym. spec.	
IR	Raman	IR	Raman	IR	Raman[b]	IR	Raman		C_{3v}	C_{2h}
2989 m	2984 m	2961 m	2966 m	2968 m	2961 m	2961 m	2962 s	Re−CH_3 asym. str.	e	
2900 m	2902 w	–	2905 s	–	2914 sh	–	2907 s	Re−CH_3 sym. str.	a_1	
			2899 sh		2902 s					
1374 w	1375 w,dp					1378 s	1379 w, sh	CH_3 asym. def.	e	
					1382 w, dp			CH_3 asym. def.		a_g/b_g
		1378 s		1378 s				CH_3 asym. def.		a_u/b_u
		1378 s						Re=N asym. str.		b_u
			1338 vs					Re=N sym. str.		a_g
						1333 s	1333 vs	$Re(=N)_3$ asym. str.	e	
				1333 s	1333 sh, dp			$Re(=N)_2$ asym. str.		a_g/b_u
						1290 m	1291 s	$Re(=N)_3$ sym. str.	a_1	
					1298 m, p			$Re(=N)_2$ sym. str.		a_g
				1290 s				$Re(=N)_2$ asym. str.		b_u
1207 w	1206 vw.p					1229 w	1227 w, m	CH_3 sym. def.	a_1	
		1227 m		1229 m				CH_3 sym. def.		b_u
			1225 m		1227 m, p			CH_3 sym. def.		a_g
998 vs	995 vvs,p							ReO_3 sym. str.	a_1	
959 vvs	960 m,dp							ReO_3 asym. str.	e	
		950 vs						ReO asym. str.		b_u
			948 w					ReO sym. str.		a_g
740 m	736 w					748 s	745 sh	CH_3 rock	e	
			740vw		759 w, dp			CH_3 rock		a_g/b_g
		746 s		749 s				CH_3 rock		a_u/b_u
			725 m		725 w,dp			Re−O−Re str.		a_g
		703 vs		681 vs				Re−O−Re str.		b_u
567 w	572 w,p					538 w, m	537 m	Re−CH_3 str.	a_1	
		541 w		539 w, m				Re−CH_3 str.		b_u
			533 w, m		524 m, p			Re−CH_3 str.		a_g
		461 sh	461 sh		463 w, dp		464 wm	*6c* imido ligand		
		450 w	457 w	456 w		456 w				
			439 w	439 w	439wm, p	439 w	437 m	*6a* imido ligand		
				426 w		425 w				
				394 w						
		370 vw	387 sh		370 sh					
		357 w		355 w		359 w		*18b* imido ligand		
				347 vw						
325 w	315 s, dp	333 w						ReO_3, ReO_2 deform.	e	b_u
						330 vw	329 m	ReN_3 deform.	e	
		302 w	305 m	311 w	308 m, p	307 w		ReN, ReN_2, ReN_3 deform	a_1	
							297 s	ReN_3 rock	e	
		291 sh		281 rw	298 sh			(*15* imido ligand)		
								ReN, ReN_2 deform.		
						268 vw				
						256 vw				
				263 w	256 w, p	248 vw	254 m	*9a* imido ligand		
			251 w, m	253 w	251vw			Re−O−Re deform.		
254 s	248 s, dp	243w	239 sh					ReO_3, ReO_2 rock		
		227w			226 m, p	215 vw	224 vw	*10a* imido ligand		
		189 vw	183 vw		196 w			Re−O−Re deform.		
		165 vw		170 vw	169 vw	169 vw	178 vw			
			148 sh	156 vw	156 sh					
				148 w	148 sh					
			134 m	134 w, m	134 m		134 s	*17b* imido ligand		

[a] From ref.[10] − [b] Depolarization ratios from solution Raman spectra, but all other frequencies for solid samples.

to allow for a systematic comparison, we have also calculated the vibrations of N-bridged dimers.

In Figure 5 we present the approximate normal modes ν_1 to ν_4 that involve a movement of the bridging atom; the corresponding calculated vibrational frequencies are collected in Table 3. The frequencies range from 470 to 750 cm^{-1}, and the largest occurs in the oxygen-bridged dimer $\mathbf{A_{O,O}(1-1)trans}$. An exception is vibration ν_4 which is similar for the dimers $\mathbf{A_{O,O}(2b-2b)trans}$, $\mathbf{A_{O,O}(3a-3a)trans}$, and $\mathbf{A_{O,O}(3b-3b)trans}$, but with slightly larger frequencies. N-Bridged dimers tend to exhibit higher frequencies than their O-bridged congeners. For $\mathbf{A_{N,N}(2a-2a)trans}$, ν_2 has a higher frequency than ν_1, in contrast to the other complexes. The frequencies ν_2 and ν_4 of $\mathbf{A_{N,N}(2a-2a)trans}$ couple to a N−CH_3 stretching mode, thus splitting into higher and lower frequency modes.

The experimental IR and Raman bands observed for compound **5c** at 950 cm^{-1} and 948 cm^{-1} demonstrate the presence of terminal oxygen atoms bonded to the rhenium center. It was not possible to assign a band to an Re−N−Re bridging structure of compounds **5c** and **6c**. Also for **4c** we were unable to identify a bridging NR unit, thus indicating the absence of such dimers. This is in agreement with the calculated results that the formation of N-

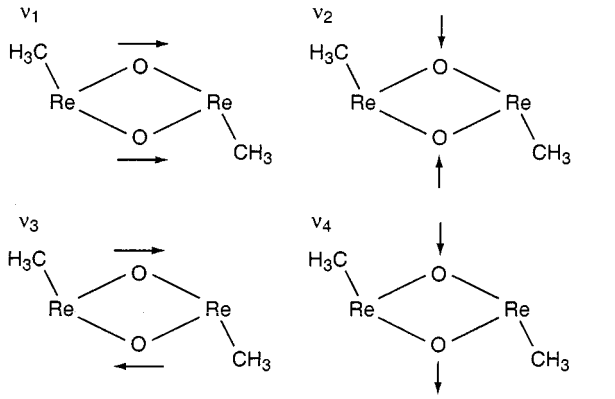

Figure 5. Sketch of the characteristic normal modes of the bridging unit Re−X−Re

Table 3. Calculated Re−X−Re frequencies $\nu_1-\nu_4$ of various dimers (in cm^{-1})

	ν_1[a]	ν_2[a]	ν_3[a]	ν_4[a]
$A_{O,O}$(1−1)trans	738.8	723.2	596.0	522.7 471.5[b]
$A_{N,N}$(2a−2a)trans	744.7	756.5	640.1	567.0
$A_{N,N}$(2b−2b)trans	753.2	480.5 1122.3[c]	679.3	395.7 1056.8[c]
$A_{O,O}$(2a−2a)trans	708.3	694.9	572.0	485.5
$A_{O,O}$(2b−2b)trans	718.5	687.4	557.5	535.9 493.8[b]
$A_{O,O}$(3a−3a)trans	728.6	679.6	563.8	520.7 479.9[b]
$A_{O,O}$(3b−3b)trans	700.4	667.8	541.5	527.0 575.6[b]
$A_{C,C}$(7−7)trans	639.7	548.2	644.5	467.4

[a] See Figure 6 for sketches of the corresponding normal modes. − [b] Vibration couples to Re−C stretching vibration, and thus splits into symmetric and antisymmetric contributions. − [c] Vibration coupled to the N−CH_3 stretching vibration; the modes with higher frequencies exhibit a larger N−CH_3 contribution.

bridged dimers with bulky substituents is endothermic. In a nitrogen-bridging structure, compound **6c** should show strong stretching features for Re=O bonding. However, such features are completely missing from the vibrational spectra (Table 2).

We also did not observe a mixture of monomeric and dimeric molecules in the case of complexes **5c** and **6c** in the solid state. Only dimeric compounds seem to be present under these particular conditions. This question had remained unsettled since our first synthesis of these complexes and their identification as dimers by X-ray crystallography.[5] It had not been possible to exclude the simultaneous presence of both monomeric and dimeric forms in the solid state, but only dimers crystallize easily. Previously, we showed that a temperature-dependent monomer−dimer equilibrium can be observed by NMR spectroscopy in solution.[5]

Assignment of the spectral region below 500 cm^{-1} is rather complicated since a number of features are characteristic of 1,2,3-substituted aromatic ring vibrations. The imido ligand exhibits local C_{2v} symmetry, and therefore the polarized Raman bands have a_1 character. Consequently the polarized lines of compound **6c** at 439, 256, and 226 cm^{-1} can be assigned to modes *6a*, *9a*, and *10a*, respectively. This Wilson notation (italicized numbers) of the aromatic ring vibrations of the (2,6-diisopropylphenyl)imido ligand was chosen according to ref.[13]

It is interesting to compare the strengths of Re=O and Re−CH_3 bonds of different complexes[7] using the stretching frequencies as a probe for the bond strength. In CH_3ReO_3, the Re=O stretching frequencies ν(Re=O) are 997 cm^{-1} and 954 cm^{-1} for the symmetric and asymmetric vibrations, respectively. The Re=O bond length is 1.705 Å. For the dimeric compound **5c**, ν(Re=O) is 950 cm^{-1} and 948 cm^{-1} (for the symmetric and antisymmetric vibrations, respectively) and the Re=O bond length is 1.702 Å. According to these values, substitution of an oxo ligand of MTO by an imido group (or several such substitutions), and subsequent dimerization leads to a weakening of the Re=O bonds.

However, not only is the Re=O bond weakened owing to substitution of oxo groups by imido groups, but the Re−C bond also changes. Figure 6a shows how the Re−C stretching frequencies vary with the corresponding bond lengths based on experimental (filled symbols) and calculated data (open symbols). Calculated values differ from the corresponding experimental values (Table 4). For CH_3ReO_3 (**1**), *d*(Re−C) was measured to be 2.060 Å, while we calculated 2.090 Å. In accordance with this longer bond, the corresponding stretching frequency is lower (exp.: 574 cm^{-1}; calcd.: 550 cm^{-1}). For the other complexes investigated experimentally (**4c**, **5c**, and **6c**), we may compare the model systems **4b**, **$A_{O,O}$(2b−2b)trans** and **$A_{O,O}$(3b−3b)trans**. Here also, the calculated bonds tend to be weaker, as judged by an overestimation of the bond lengths [by 0.026 Å in **4b**, 0.008 Å in **$A_{O,O}$(2b−2b)trans**, and 0.021 Å in **$A_{O,O}$(3b−3b)trans**] and an underestimation of the corresponding stretching frequencies. These calculated data fit the same essentially linear relationship between bond lengths and frequencies as the experimental data (Figure 6a). The MTO dimer and the N-bridged imido dimer are the only exceptions (open diamonds, Figure 6a). Figure 6b shows the calculated stretching frequencies as a function of the natural atomic charge of the rhenium center. For the monomers **1**, **2a/b**, **3a/b**, and **4a/b**, we conclude that with increasing electron deficiency at the metal center, i.e. with higher positive charge *q*(Re) (Figure 6b), the Re−C bond becomes shorter and more rigid (higher vibrational frequency). The dimers do not fit that linear correlation. The effect of rehybridization on the metal center due to dimerization causes more complex changes in the electronic structure which, in turn, affects the Re−C bond.

Ligand Exchange between Monomers

Finally, we discuss the energies of group-exchange reactions between two monomers, which occur via a dimer structure. We will start by discussing a possible reaction coordinate. Symmetry is a key point for rationalizing this exchange problem. If we assume a synchronous process, the reaction pathway has to pass a structure where both M−X bonds of each bridging atom X are equivalent by symmetry.

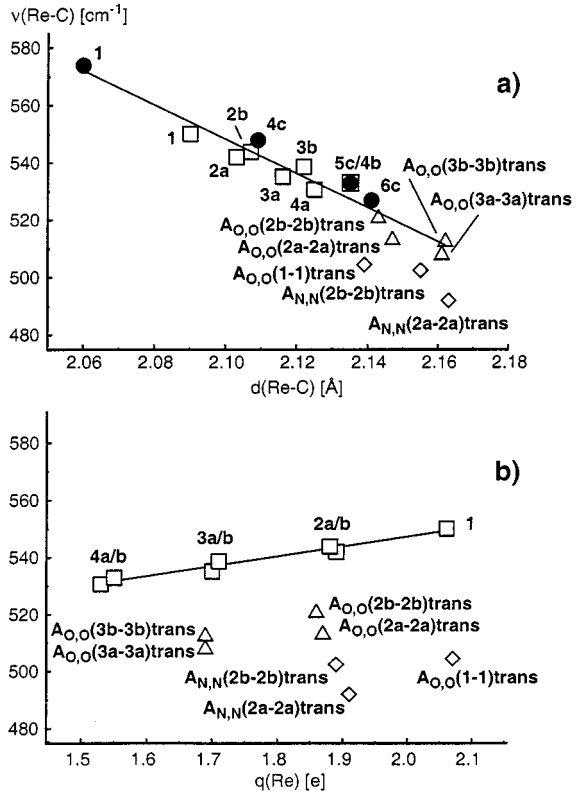

Figure 6. Experimental (filled circles) and calculated (open symbols) Re−C stretching frequencies ν(Re−C) as a function of (a) the Re−C bond length *d*(Re−C); and (b) the calculated natural atomic charges *q*(Re) of Re (in e); for the calculated data, the most stable conformers were used (monomers − open squares, O-bridged dimers − open triangles, MTO dimer and N-bridged dimers − open empty diamonds)

Table 4. Calculated and experimental Re−C bond lengths (in Å) and stretching frequencies (in cm^{-1}) for various monomers and dimers; also shown are the corresponding calculated natural atomic charge *q*(Re) (in e)

	d(Re−C)	ν(Re−C)	*q*(Re)
Monomers:			
1	2.090	550.2	2.06
1[a]	2.060	574	
2a	2.103	542.1	1.89
2b	2.107	544.0	1.88
3a	2.116	535.3	1.70
3b	2.122	538.8	1.71
4a	2.125	530.8	1.53
4b	2.135	533.1	1.55
4c[a]	2.135	541, 533	
Dimers:			
$\mathbf{A_{O,O}(1-1)trans}$	2.139	504.6	2.07
$\mathbf{A_{N,N}(2a-2a)trans}$	2.163	492.1	1.91
$\mathbf{A_{N,N}(2b-2b)trans}$	2.155	502.6	1.89
$\mathbf{A_{O,O}(2a-2a)trans}$	2.147	513.7	1.87
$\mathbf{A_{O,O}(2b-2b)trans}$	2.143	521.3	1.86
$\mathbf{A_{O,O}(3a-3a)trans}$	2.161	508.5	1.69
$\mathbf{A_{O,O}(3b-3b)trans}$	2.162	513.1	1.69
5c[a]	2.141	539, 527	
6c[a]	2.109	548	

[a] Experimental values.

This structure can be a transition state, but it could also be a stable or metastable intermediate (see Figure 7). In the first case the reaction coordinate features one transition structure that interconnects two local equilibrium points of the potential-energy surface (PES). Each of the atoms can be assigned to a certain metal center. The final structure can either be two isolated molecules, or a dimer which has two bridging atoms X with two different M−X bond lengths. If the structure with the symmetry-equivalent M−X bonds is a (meta)stable intermediate, then the reaction path has two saddle points which lie between the symmetric local minimum structure and the structure where each atom X is uniquely assigned to only one metal center.

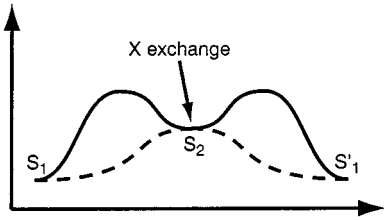

Figure 7. Sketch of the potential-energy surface for the exchange of group X in dimers at the stationary point S_2; the stationary points S_1 and S_1' indicate configurations in which the groups X can be assigned to one of the metal centers, either in the case of two monomers or in the case of a dimer with asymmetric bridges; the solid line represents an energy profile with S_2 as (meta)stable intermediate, the dashed line represents an energy profile with S_2 as transition state

In the following discussion of ligand-exchange reactions, we will restrict ourselves to the special case of oxygen-bridged dimers. For ligand-exchange reactions of MTO and related dimers, we can discriminate four pertinent structures which can be (meta)stable intermediate dimers or transitions states, or stable dimers in which each bridging atom X belongs to one metal center only.

Only structure $\mathbf{A_{O,O}(1-1)trans}$ exhibits two different M−X bonds, while the structures $\mathbf{A_{O,O}(1-1)cis}$, $\mathbf{B_{O,O}(1-1)cis}$ and $\mathbf{B_{O,O}(1-1)trans}$ can either be (meta)-stable intermediates, or transition states. From frequency calculations, one discovers that *cis* and *trans* structures **B** are both third-order saddle points, and thus not proper transition states. On the other hand, *cis* and *trans* configurations of structure **A** are both metastable.

The optimized transition state (see Figure 8) of the oxygen exchange reaction corresponds to a complex reaction coordinate. The barrier height $\Delta E^{\neq}$ is 23.8 kcal/mol ($\Delta H^{\neq}$ = 24.4 kcal/mol). It connects two isolated MTO complexes (lower-energy asymptote in Figure 7) with dimer structure $\mathbf{A_{O,O}(1-1)trans}$, which is thus identified as a metastable intermediate (Figure 7). The dimerization energy ΔE of this intermediate is 1.7 kcal/mol (ΔH = 3.5 kcal/mol, see Table 1). To facilitate the understanding of the three-dimensional structure of the transition state, we display two orientations of this structure in Figure 8. The arrows indicate the motion of the nuclei along the reaction coordinate in the direction in which the metastable intermediate $\mathbf{A_{O,O}(1-1)trans}$ is formed. Note that the order of the Re−O bond lengths in the bridging unit is reversed in comparison to the dimeric compound (see Figure 1). The shorter Re−O bond in the transition state (1.835 Å; Fig-

ure 8) is the one closer to the Re−C bond, which is 2.046 Å in the dimer [see Figure 1, (a)]. The longer bond in the transition structure (2.208 Å, Figure 8) is *trans* to the methyl group; it corresponds to the shorter bridging bond, 1.902 Å (Figure 1), of the dimer. These changes demonstrate the exchange of the two oxygen atoms through the formation of a dimer. In the transition state, the two carbon−rhenium bonds do not fall in one plane, in contrast to the dimer structure; the dihedral angle C−Re−Re−C is 115°. The nuclear motion along the reaction coordinate does not only comprise an exchange of oxygen centers, but also a rotation of each monomer around the shorter Re−O bridging bond in the transition state. However, the transition structure exhibits C_2 symmetry, with the rotation axis perpendicular to the plane that contains the Re−O bridging bonds.

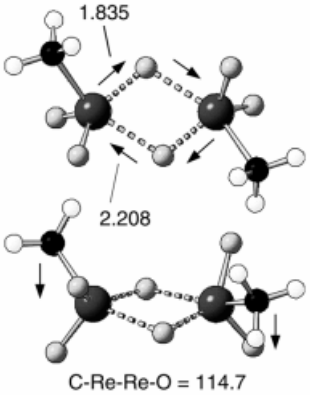

Figure 8. Calculated transition-state structure of oxygen exchange in the dimer $\mathbf{A_{O,O}(1-1)trans}$; top: view onto the Re−O−Re plane; bottom: Re−O−Re plane rotated around the Re−Re axis; arrows indicate motions of the nuclei along the reaction coordinate from the transition state to the metastable intermediate $\mathbf{A_{O,O}(1-1)trans}$; bond lengths in Å, angles in °

Conclusions

The most stable dimers of oxo, imido, and mixed imido/oxo alkylrhenium(VII) complexes display a trigonal-bipyramidal structure at the metal centers, with a *trans* arrangement of the methyl ligands. While the *cis* arrangement of the methyl ligands leads only to slightly higher energies (about 5 kcal/mol), pseudo square-pyramidal arrangements have a considerably higher energy (about 30 kcal/mol) than trigonal-bipyramidal structures. This is in good agreement with published structures, but contrasts with previously published HF calculations concerning the first step of the polymerization of methyltrioxorhenium(VII). In all cases examined, the stabilization gained by the dimerization process is rather small (usually < 5 kcal/mol), explaining the ease of the Re−O−Re bond cleavage and reformation during the sublimation process of the compounds **2** ⇄ **5** and **3** ⇄ **6**. In some cases, most notably for methyltrioxorhenium(VII), the dimerization process is (slightly) endothermic, according to our calculations. Therefore, dimers cannot be isolated but are likely to be present as short-lived species. This explains the ease of reversible oxygen-transfer reactions between O-labeled and -unlabeled organorhenium(VII) oxides which have often been observed,[8] even in water-free solvents. Based on the present results, we suggest that these processes proceed via (short-lived) oxygen bridges.

According to our calculations, N-bridged dimers of the compounds **2**−**4** should be stable. At first glance, this seems to contradict our vibrational spectroscopy results, which show no indication for N-bridged species whatsoever. However, our calculations were performed with N−H and $N-CH_3$ species as bridging groups and have already shown that dimer formation becomes more endothermic when N−H groups are substituted by $N-CH_3$ species. However, imido and mixed imido/oxo complexes with N−H or $N-CH_3$ groups are too unstable to be isolated.[4] The bulky ligands we used in an attempt to isolate imido or oxo/imido species evidently disfavor dimers significantly more than do CH_3 groups, thus resulting in monomers such as **4** becoming the energetically preferred species.

Experimental Section

All preparations and manipulations were performed with standard Schlenk techniques under oxygen- and water-free argon. Solvents were dried by standard procedures: THF, Et_2O, *n*-pentane, and *n*-hexane with Na/benzophenone ketyl. Acetonitrile and dichloromethane were distilled after heating at reflux for several hours over P_2O_5. Acetone was distilled from K_2CO_3 and kept over 4-Å molecular sieves. − The TG/MS studies were carried out with a Perkin−Elmer TGA 7 thermobalance coupled with a Balzers QMG 420 mass spectrometer. The thermolysis experiments were carried out in a dynamic helium environment (purity 5.0, 45 sccm) using a 50−600 °C temperature program at a rate of 10 °C/min. The temperature of the capillary interface was 280 °C. TG studies were additionally performed using a Shimadzu TGA-50 thermobalance. The experiments were carried out under nitrogen at 25−1000 °C, at a rate of 5 °C/min from room temperature to 1000 °C, using a platinum cell. − The Raman spectra were recorded with a Bio-Rad dedicated FT-Raman spectrometer using the near-infrared excitation 1064 nm of a Nd:YAG diode laser. − The infrared spectra in the 4000−200 cm^{-1} region were recorded using a Bio-Rad FTS-175 spectrometer equipped with CsI-based beam splitter, and the far-infrared (400−50 cm^{-1}) measurements were carried out with the same spectrometer, but using a 6-μm Mylar beam-splitter. − The compounds CH_3ReO_3 (**1**), $[CH_3ReO_2(NR)]_2$ (**5c**), $[CH_3ReO(NR)_2]$ (**6c**), and $CH_3Re(NR)_3$ (**4c**) (with R = 2,6-diisopropylphenyl) were prepared according to published procedures.[5,14]

Computational Details: All electronic structure calculations were performed with the hybrid B3-LYP[15] density-functional scheme,[16] using effective-core potentials for rhenium with a partly decontracted basis set for rhenium.[17] Geometry optimizations were carried out using a 6-311G(d,p) basis[18] on all centers (except Re). Enthalpies were calculated at this level following standard procedures.[19] Finally, two f exponents[3e,7] were added to the basis set of Re to evaluate energies in a single-point fashion. Details of this computational strategy have been discussed elsewhere.[7] Transition-state structures were verified to feature only one imaginary frequency in the vibrational spectrum. Additionally, by following

the transition vector, we verified that the reaction products and reactants are directly reached from the transition structure.[20]

Acknowledgments

F. E. K. is greatly indebted to Prof. Dr. W. A. Herrmann for continuous support. This work was supported by the DAAD (Accões Integradas and Keretében Megvalósuló Program), the BMFT/JNICT Protokoll, the Deutsche Forschungsgemeinschaft, and the Fonds der Chemischen Industrie.

[1] W. A. Herrmann, F. E. Kühn, G. M. Lobmeier, in: *Aquous Phase Catalyis* (Eds.: B. Cornils, W. A. Herrmann), VCH-Wiley, Weinheim, New York, **1998**.

[2] Recent reviews: [2a] W. A. Herrmann, F. E. Kühn, *Acc. Chem. Res.* **1997**, *130*, 1169. – [2b] F. E. Kühn, R. W. Fischer, W. A. Herrmann, *Chem. Unserer Zeit* **1999**, *33*, 192. – [2c] F. E. Kühn, W. A. Herrmann, *Struct. Bonding* **2000**, *97*, 211.

[3] [3a]T. Szyperski, P. Schwerdtfeger, *Angew. Chem. Int. Ed. Engl.* **1989**, *28*, 1128. – [3b] R. Wiest, T. Leininger, G. H. Jeung, M. Bénard, *J. Phys. Chem.* **1992**, *96*, 10800. – [3c] S. Köstlmeier, O. D. Häberlen, N. Rösch, W. A. Herrmann, B. Solouki, H. Bock, *Organometallics* **1996**, *15*, 1872. – [3d] S. Köstlmeier, V. A. Nasluzov, W. A. Herrmann, N. Rösch, *Organometallics* **1997**, *16*, 1786. – [3e] P. Gisdakis, S. Antonczak, S. Köstlmeier, W. A. Herrmann, N. Rösch, *Angew. Chem. Int. Ed.* **1998**, *37*, 2211. – [3f] C. Mealli, J. A. Lopez, M. J. Calhorda, C. C. Romão, W. A. Herrmann, *Inorg. Chem.* **1994**, *33*, 1139. – [3g] A. Gobbi, G. Frenking, *J. Am. Chem. Soc.* **1994**, *116*, 9275.

[4] [4a] C. J. Longley P. D. Savage, G. Wilkinson, B. Hussain, M. Hursthouse, *Polyhedron* **1988**, *7*, 1079. – [4b] A. D. Horton, R. R. Schrock, J. H. Freundenberger, *Organometallics* **1987**, *6*, 893. – [4c] D. S. Williams, R. R. Schrock, *Organometallics* **1993**, *12*, 1148. [4d] M. R. Cook, W. A. Herrmann, P. Kiprof, J. Takacs, *J. Chem. Soc., Dalton Trans.* **1991**, 797. – [4e] A. Gutierrez, G. Wilkinson, B. Hussain-Bates, M. B. Hursthouse, *Polyhedron* **1990**, *9*, 2081. – [4f] W. A. Herrmann, G. Weichselbaumer, R. A. Paciello, R. A. Fischer, E. Herdtweck, J. Okuda, D. W. Marz, *Organometallics* **1990**, *9*, 489. – [4g] W. D. Wang, J. H. Espenson, *Organometallics* **1999**, *18*, 5170.

[5] W. A. Herrmann, H. Ding, F. E. Kühn, W. Scherer, *Organometallics* **1998**, *17*, 2751.

[6] [6a] W. A. Herrmann, R. W: Fischer, *J. Am. Chem. Soc.* **1995**, *117*, 3223. – [6b] H. S. Genin, K. A. Lawler, R. Hoffmann, W. A. Herrmann, R. W: Fischer, W. Scherer, *J. Am. Chem. Soc.* **1995**, *117*, 3244. – [6c] S. Köstlmeier, G. Pacchioni, W. A. Herrmann, N. Rösch, *J. Organomet. Chem.* **1996**, *514*, 111. – [6d] W. A. Herrmann, W. Scherer, R. W. Fischer, J. Blümel, M. Kleine, W. Mertin, R. Gruehn, J. Mink, H. Boysen, C. C. Wilson, R. M. Ibberson, L. Bachmann, M. Mattner, *J. Am. Chem. Soc.* **1995**, *117*, 3231.

[7] P. Gisdakis, S. Antonczak, N. Rösch, *Organometallics* **1999**, *18*, 5044.

[8] [8a] W. A. Herrmann, F. E. Kühn, P. W. Roesky, *J. Organomet. Chem.* **1995**, *485*, 243. – [8b] W. A. Herrmann, F. E. Kühn, M. U. Rauch, J. D. G. Correia, G. R. J. Artus, *Inorg. Chem.* **1995**, *34*, 2914. – [8c] W. A. Herrmann, J. D. G. Correia, M. U. Rauch, G. R. J. Artus, F. E. Kühn, *J. Mol. Catal.* **1997**, *118*, 33. – [8d] W. A. Herrmann, W. A. Wojtczak, G. R. J. Artus, F. E. Kühn, M. R. Mattner, *Inorg. Chem.* **1997**, *36*, 465.

[9] W. A. Herrmann, W. Wachter, F. E. Kühn, R. W. Fischer, *J. Organomet. Chem.* **1998**, *553*, 443.

[10] J. Mink, G. Keresztury, A. Stirling, W. A. Herrmann, *Spectrochim. Acta* **1994**, *50A*, 2039.

[11] W. A. Herrmann, J. G. Kuchler, J. K. Felixberger, E. Herdtweck, W. Wagner, *Angew. Chem. Int. Ed. Engl.* **1988**, *27*, 394.

[12] W. A. Herrmann, M. Flöel, J. Kulpe, J. K. Felixberger, E. Herdtweck, *J. Organomet. Chem.* **1988**, *355*, 297.

[13] G. Varsányi, *Assignment for Vibrational Spectra of 700 Benzene Derivatives*, Akadémia Kiadó, Budapest, **1973**, pp. 298.

[14] W. A. Herrmann, R. Kratzer, R. W. Fischer, *Angew. Chem. Int. Ed. Engl.* **1997**, *36*, 2652.

[15] [15a] A. D. Becke, *J. Chem. Phys.* **1993**, *98*, 5648. – [15b] C. Lee, W. Yang, R. G. Parr, *Phys. Rev. B* **1988**, *37*, 785.

[16] M. J. Frisch, G. W. Trucks, H. B. Schlegel, P. M. W. Gill, B. G. Johnson, M. A. Robb, J. R. Cheeseman, T. Keith, G. A. Petersson, J. A. Montgomery, K. Raghavachari, M. A. Al-Laham, V. G. Zakrzewski, J. V. Ortiz, J. B. Foresman, J. Cioslowski, B. B. Stefanov, A. Nanayakkara, M. Challacombe, C. Y. Peng, P. Y. Ayala, W. Chen, M. W. Wong, J. L. Andres, E. S. Replogle, R. Gomperts, R. L. Martin, D. J. Fox, J. S. Binkley, D. J. Defrees, J. Baker, J. P. Stewart, M. Head-Gordon, C. Gonzalez, J. A. Pople, *Gaussian 94, Revision D.4*, Gaussian Inc., Pittsburgh PA, USA, **1995**.

[17] [17a] P. J. Hay, W. R. Wadt, *J. Chem. Phys.* **1985**, *82*, 299. [17b] G. Frenking, I. Antes, M. Böhme, S. Dapprich, A. W. Ehlers, V. Jonas, A. Neuhaus, M. Otto, R. Stegmann, A. Veldkamp, S. F. Vyboishchikov, in: *Reviews in Computational Chemistry*, vol. 8 (Eds.: K. B. Lipkowitz, D. B. Boyd), VCH, New York, **1996**, p. 63.

[18] R. Krishnan, J. Binkley, R. Seeger, J. Pople, *J. Chem. Phys.* **1980**, *72*, 650.

[19] W. J. Hehre, L. Radom, P. v.R. Schleyer, J. A. Pople, *Ab initio Molecular Orbital Theory*, Wiley, New York, **1986**.

[20] Internal reaction coordinate analysis carried out at the LanL2DZ level; cf. ref.[17]; see also: C. Gonzalez, H. B. Schlegel, *J. Chem. Phys.* **1990**, *94*, 5523.

Received September 27, 2000
[I00363]